Surface cloud warming increases as Fall Arctic sea ice cover decreases

Assia Arouf[1], Hélène Chepfer[1], Jennifer E. Kay[2,3], Tristan S. L'Ecuyer[4], Jean Lac[1]

[1]LMD/IPSL, Sorbonne Université, École Polytechnique, Institut Polytechnique de Paris, ENS, PSL Université, CNRS, Palaiseau, France
[2]CIRES, University of Colorado Boulder, Boulder, USA
[3]ATOC, University of Colorado Boulder, Boulder, USA
[4]Department of Atmospheric and Oceanic Sciences, University of Wisconsin-Madison, Madison, USA

Key Points:

- During October, large surface cloud warming with values higher than 80 W m^{-2} occurs ∼+50% more often over open water than over sea ice.
- Compared to October, November large surface cloud warming (> 80 W m^{-2}) occurs even more frequently (∼+200%) over open water than over sea ice
- More frequent large surface warming caused by low-level opaque clouds occurs as open water persists later into the fall.

Corresponding author: Assia Arouf, assia.arouf@lmd.ipsl.fr

Abstract

During the Arctic night, clouds regulate surface energy budgets through longwave warming alone. During fall, any increase in low-level opaque clouds will increase surface cloud warming and could potentially delay sea ice formation. While an increase in clouds due to fall sea ice loss has been observed, quantifying the surface warming is observationally challenging. Here, we quantify surface cloud warming using spaceborne lidar observations. By instantaneously co-locating surface cloud warming and sea ice observations in regions where sea ice varies, we find October large surface cloud warming values ($> 80\,\mathrm{W\ m^{-2}}$) are much more frequent ($\sim$+50%) over open water than over sea ice. Notably, in November large surface cloud warming values ($> 80\,\mathrm{W\ m^{-2}}$) occur more frequently ($\sim$+200%) over open water than over sea ice. These results suggest more surface warming caused by low-level opaque clouds in the future as open water persists later into the fall.

Plain Language Summary

Over the past 40 years, Arctic sea ice has experienced an extreme decline, leaving a large surface of open water and an increased surface temperature. Through their impact on energy budgets, clouds have the potential to increase or decrease sea ice decline. More low-level clouds over open water than over sea ice during non-summer seasons have already been observed. But quantifying their radiative effect remains challenging. Therefore, this study seeks to answer the following question: By how much fall Arctic clouds can change surface warming in response to sea ice loss? Using high temporal and geographical space-based observations, we found that large surface cloud warming, higher than $80\,\mathrm{W\ m^{-2}}$, occurs much more frequently over open water than over sea ice during October and November months. This suggests that Arctic clouds favor sea ice loss by delaying sea ice recovery. As the Arctic continues to warm up due to human activities, cloud surface warming will delay sea ice freeze-up later into the fall and may amplify Arctic sea ice loss.

1 Introduction

Over the past 40 years, the Arctic has experienced the largest warming on Earth (Serreze & Barry, 2011). Specifically, the Arctic has warmed nearly four times faster than the global average (Rantanen et al., 2022) and also lost sea ice, especially in late summer and early fall since the satellite record began (Stroeve et al., 2012). More summer melt and a longer melt season lead to more shortwave (SW) absorption in the Arctic ocean and greater ocean warming (Manabe & Stouffer, 1980). Warmer and larger areas of open water during longer duration can influence the adjacent ice cover, contributing to further thinning and delaying sea ice freeze-up (Stroeve et al., 2012, 2014).

On the other hand, enhanced surface longwave (LW) warming due to increased water vapor and cloudiness may accelerate sea ice melt in early spring (Huang et al., 2019) and would delay sea ice freeze-up in fall (Morrison et al., 2018), resulting in a longer melt season. Air-sea coupling during non-summer season promotes the formation of low-level liquid clouds above open water in response to sea ice loss (Kay & Gettelman, 2009). These low-level clouds affect surface radiative fluxes and may affect sea ice formation. Indeed, clouds radiatively warm the surface in the LW by trapping upward LW earth surface radiation that would otherwise escape the earth system. Conversely, they radiatively cool the surface in the SW by reflecting solar radiation back to space. During Arctic summer over the ocean, the SW effect dominates over the LW effect and clouds cool the surface. In all other seasons, clouds warm the surface and may enhance sea ice loss. On average overall, Arctic clouds warm the ocean surface (Kay & L'Ecuyer, 2013).

In fall, Morrison et al. (2018) using 8 years of local instantaneous spaceborne lidar observations, found more low-level clouds over open water than over sea ice. But,

quantifying the surface radiative impact of these low-level clouds formed over newly open water is challenging. Therefore, this study investigates to answer the following questions: i) By how much fall Arctic clouds can change surface LW warming in response to sea ice cover changes? ii) How do they evolve through fall? Due to the limited availability of ground-based observations in the Arctic, satellite observations are unquestionably needed for investigating changes in the Arctic climate system. As low-level clouds exert a large surface warming effect (Arouf, Chepfer, Vaillant de Guélis, Chiriaco, et al., 2022; Matus & L'Ecuyer, 2017; Shupe & Intrieri, 2004), we need to accurately observe them above sea ice and open water to detect surface cloud warming changes in response to Arctic sea ice variability. Spaceborne Active sensors are good candidates as they sample vertically the atmosphere above all surface types, including sea ice and open water, providing consistent cloud observations at relatively long time periods with near-global spatial coverage (Stubenrauch et al., 2013). We use spaceborne lidar observations at a local instantaneous resolution to quantify the warming effect induced by low-level liquid clouds formed over newly open water during fall. We use 13 years of Cloud–Aerosol Lidar and Infrared Pathfinder Satellite Observations (CALIPSO; Winker et al., 2010) observations between 2008 and 2020, a period with a large sea ice loss and a large sea ice concentration interannual variability (Serreze & Meier, 2019).

2 Data

Cloud data used in this study are based on CALIPSO spaceborne lidar observations with a high spatiotemporal resolution (HSTR; 90 m cross track, 330 m along orbit track). CALIPSO data are surface type independent, *i.e.* accurate observations over sea ice and over open water, unlike spaceborne radiometers that are dependent on the background surface type to detect clouds and are limited over icy bright surfaces. Moreover, space lidar samples the atmosphere and observes clouds at all atmosphere levels, except the ones under the altitude where the space lidar is fully attenuated. We use 13 years (2008–2020) of CALIPSO observations which allows having a large area where Arctic sea ice cover varies during fall, with almost half of CALIPSO's profiles over sea ice and the other half over open water. We use cloud data from GCM Oriented CALIPSO Cloud Product (CALIPSO–GOCCP v3.1.2; Chepfer et al., 2010; Cesana et al., 2012; Guzman et al., 2017; Vaillant de Guélis et al., 2017). Space lidar differentiates well cloud types and each profile is classified (*Profile-flag*) as *Clear sky* when no cloud is detected; *Thin cloud* when clouds and surface echo are detected; *Opaque cloud* when clouds, with visible optical depth $>$ 3−5 depending on the cloud's microphysical properties (Chepfer et al., 2014), are detected but no surface echo is detected (Guzman et al., 2017); *Uncertain* in all other cases (*e.g.* surface echo not detected and no fully attenuated altitude detected). When a cloud is detected, we can retrieve its *cloud altitude*. $Z_{T_{Opaque}}$ for opaque clouds which is the average altitude between cloud top altitude and the altitude where the space lidar gets completely attenuated in opaque clouds. $Z_{T_{Thin}}$ for thin clouds which is the average altitude between cloud top altitude and cloud base altitude.

The surface longwave cloud radiative effect (LW CRE) from LWCRE–LIDAR Edition 1 product (Arouf, Chepfer, Vaillant de Guélis, Chiriaco, et al., 2022) is used. Surface LW CRE quantifies the impact of clouds on the surface energy budget, which is the surface net radiative fluxes over all types of scenes minus the corresponding fluxes where the influence of clouds has been removed. Each lidar footprint contains either zero, for clear sky footprint, a value of surface LW Thin CRE or a value of surface LW Opaque CRE. The surface LW Opaque CRE is computed from $Z_{T_{Opaque}}$. Since the space lidar cannot observe under the altitude where the lidar is fully attenuated, it might potentially miss low-level clouds laying under this altitude. One would think that this limitation would create a large bias in the surface LW CRE retrieval and may underestimate the surface LW CRE. However, Arctic liquid clouds that are optically opaque are usually at low levels and the space lidar attenuates most of the time in the boundary layer at altitudes

lower than 3 km above the surface (Guzman et al., 2017). Uncertainties reaching $\sim$13 W m^{-2} can be induced by the lower tropospheric temperature and humidity representations and cloud base height but would not change the overall results shown in this paper.

In addition to the HSTR data, we also use gridded data: Clear sky cover, Thin cloud cover, Opaque cloud cover from GOCCP product at a monthly 1°×1° resolutions. Surface LW CRE from the LWCRE–LIDAR product at a monthly 2°×2° resolutions. Surface SW and LW CRE from the and CloudSat 2B–FLXHR–LIDAR P1–R04 (hereafter, 2BFLX; L'Ecuyer et al., 2019) product at a monthly 2.5°×2.5° resolution that is available between August 2006 through April 2011 before CloudSat experienced a battery anomaly that limited observations to daylight only. The dataset does not provide data during late fall after 2011. Uncertainties in monthly-mean surface LW fluxes from 2BFLX are $\sim$11 W m^{-2}, owing primarily to errors in lower tropospheric temperature and humidity and uncertainty in cloud base height (Henderson et al., 2013).

Sea ice concentrations are from the National Snow and Ice Data Center's Near Real-Time SSM/I EASE-Grid Daily Global Sea Ice Concentration and Snow Extent data product (NSIDC; Nolin et al., 1998). Sea ice observations, at a daily 25 km horizontal resolution, are from passive microwave imagers and have uncertainties ranging from ±5% in winter to ±15% in summer (Agnew & Howell, 2003). Each CALIPSO footprint contains a sea ice concentration value, which is assigned from the latitude/longitude closest to that satellite footprint. We also use sea ice extent at a monthly resolution between 1979 and 2021 (Fetterer et al., 2017).

3 Methods

We built surface masks following a method developed by Morrison et al. (2018) to isolate the influence of Arctic sea ice cover variability on clouds from other cloud-controlling factors. We split the Arctic, defined as the area poleward 70 °N, into two regions delimited by two masks: the perennial mask and the intermittent mask. The perennial mask isolates regions of the Arctic where the daily sea ice concentration has not changed between 2008–2020 during October months. Explicitly, this mask contains grid boxes over land including coastlines, grid boxes that remain always ice-free ($<$ 15% every day between 2008–2020), and grid boxes that remain always ice-covered ($>$ 80% every day between 2008–2020). The data over the perennial mask are excluded from our study. The intermittent mask isolates regions of the Arctic Ocean where the $1^\circ \times 1^\circ$ daily sea ice concentration has varied between 2008–2020 during October months. Specifically, the intermittent mask contains grid boxes that never remain always ice-free ($<$ 15%) nor always ice-covered ($>$ 80%). Said differently, in the intermittent mask, the daily mean sea ice concentration within a $1^\circ \times 1^\circ$ grid box is not either $<$ 15% nor $>$ 80% every single day between 2008–2020 during October months. We built another intermittent mask for November months in the same way as for October months.

Within the intermittent mask, we split the clouds into low/high, opaque/thin, over open water/over sea ice using instantaneous HSTR cloud properties for October and November months. We built low-level opaque (thin) cloud cover by dividing the number of opaque (thin) cloud profiles with mean altitudes $Z_{T_{Opaque}}$ ($Z_{T_{Thin}}$) $<$ 2 km by the total number of profiles within a 1°×1° grid box for a given month. Then we built low-level opaque cloud cover over open water only by dividing the number of opaque profiles with $Z_{T_{Opaque}}$ $<$ 2 km over open water (footprint sea ice cover $<$ 15%) by the total number of profiles over open water within a $1^\circ \times 1^\circ$ grid box for a given month. Similarly, we built the low-level opaque cloud cover over sea ice only considering the profiles with footprints of sea ice cover $>$ 80%. This classification excludes profiles containing both open water and sea ice (footprint sea ice cover $>$ 15% and $<$ 80%). In the same way, we split the surface LW CRE footprints into over open water and over sea ice and look at its distribution for opaque and thin clouds over each surface type.

This approach assumes that local processes affect more low-level clouds than large-scale patterns since clouds over open water and over sea ice are subject to the same large-scale atmospheric circulation regimes.

4 Results

October is a particularly interesting month for investigating the observed co-variability of sea ice and cloud radiative effects (Figure 1). At this time of year, the sun is setting and cloud influence on radiative fluxes is increasingly explained by the longwave cloud warming alone. In fact, from October through February, the shortwave cloud cooling is close to zero and the total cloud radiative effect is the same as the longwave cloud warming (Figure 1a). Of the months when the longwave cloud warming is the total cloud radiative effect, October has the largest Arctic sea ice loss (Figure 1b). When one compares the solid blue line (average over $2011-2021$) and the dashed pink line (average over $1979-1990$), October lost $\sim$2.8 millions of km^2 of sea ice extent during this last 40 years.

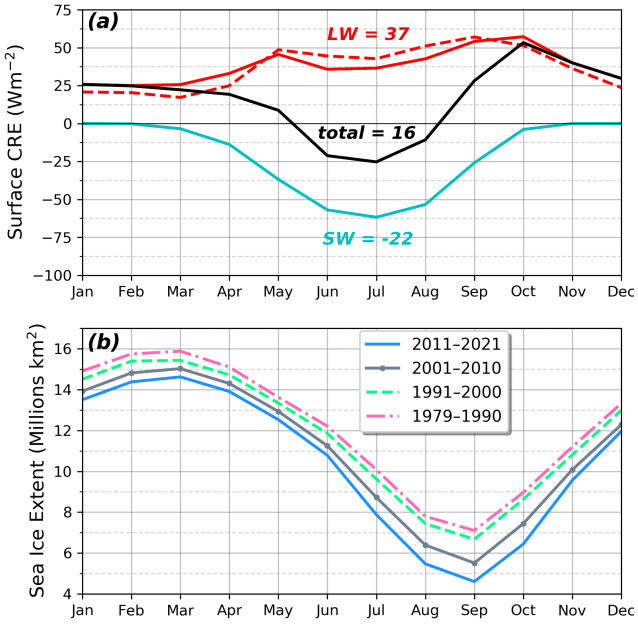

Figure 1. (a) Seasonal cycle of the surface cloud radiative effect (CRE) over Arctic oceans without northern Atlantic: longwave (LW), shortwave (SW) and total. The solid lines are from $2.5^\circ \times 2.5^\circ$ monthly 2BFLX product (L'Ecuyer et al., 2019) between 2007–2010. The dashed line is from $2^\circ \times 2^\circ$ monthly LWCRE–LIDAR product (Arouf, Chepfer, Vaillant de Guélis, Chiriaco, et al., 2022) between 2008–2020. (b) Seasonal cycles of sea ice extent.

To understand cloud-sea ice relationships in this interesting month, we map October cloud properties within the intermittent mask which isolates regions where sea ice varies (Figure 2). October is very cloudy throughout the entire intermittent mask. Averaged over intermittent mask (Figure 2b), clear sky is only present $\sim$13% of the time (Figure 2a) while clouds occur $\sim$81% of the time ($\sim$ 6% of CALIPSO's profiles within the intermittent mask are classified as uncertain). We can divide this cloud cover ($\sim$81%) into opaque and thin clouds. Furthermore, more than half of October clouds are opaque ($\sim$52%), especially at lower latitudes (Figure 2c) and half of these opaque clouds have mean altitudes under 2 km (Figure 2d) resulting in low-level opaque cloud cover of $\sim$27%.

Thin clouds dominate at higher latitudes (> 75 °N), especially in the Pacific sector of the Arctic above the Canadian Archipelago (Figure 2e) which is the coldest region of the Arctic. Most thin clouds (∼19% out of ∼29%) also have mean altitudes under 2 km.

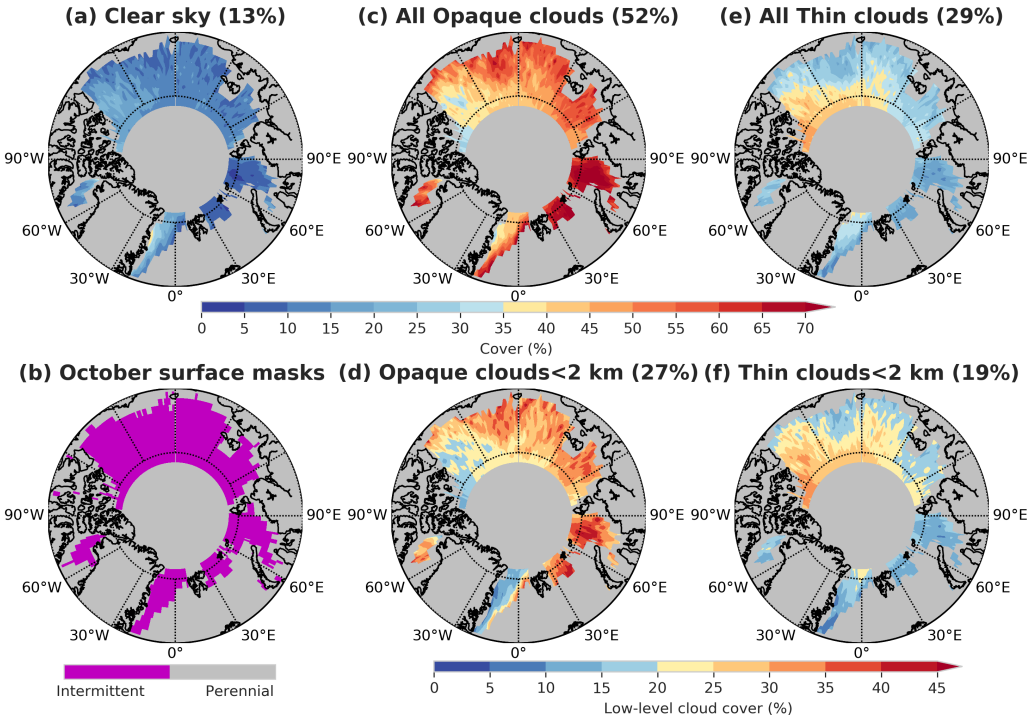

Figure 2. (a) Clear sky cover, (b) October surface masks established between 2008–2020, (c) Opaque cloud cover, (d) Low-level opaque cloud cover, (e) Thin cloud cover, (f) Low-level thin cloud cover. Data are collected during October months between 2008–2020 period from CALIPSO–GOCCP (Guzman et al., 2017) local instantaneous product. The grid boxes that have less than 100 profiles in each grid box for each October month are masked on these plots. The gray area represents the perennial mask that isolates regions of the Arctic where the 1°×1° daily sea ice concentration has not changed between 2008–2020 during October months and latitudes > 82° N where CALIPSO do not collect observations. The data over the perennial mask are excluded from our study. Every other color represents the intermittent mask that isolates regions of the Arctic Ocean where the 1°×1° daily sea ice concentration has varied between 2008–2020 during October months. Instantaneous CALIPSO–GOCCP profiles are only used within the intermittent mask. Averages established over the intermittent mask are reported in parentheses. ∼ 6% of CALIPSO–GOCCP profiles within the intermittent mask are classified as uncertain and are excluded from our study.

Low-level opaque clouds are the dominant cloud type during October months within the intermittent mask (Figure 2d; ∼27% of CALIPSO's profiles) and warm the surface more than the other clouds. Therefore, we focus on these clouds. We split these clouds into over open water and over sea ice (Figure 3). Maps show there are more low-level opaque clouds over open water than over sea ice in almost all locations. When averaged over the intermittent mask, there are ∼12% more low-level opaque clouds over open water than over sea ice. Histograms of the surface longwave cloud warming over open water and over sea ice are consistent (Figure 3c) with these low-level opaque cloud cover differences (Figure 3a–b). The largest surface longwave cloud warming values occur more

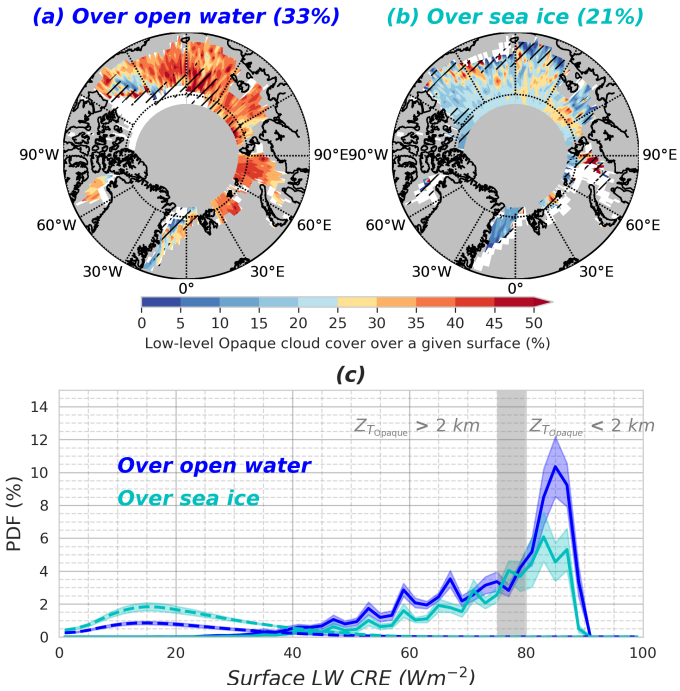

Figure 3. 1^{st} line: Maps of Low-level opaque cloud cover: (a) Over open water, (b) Over sea ice. The grid boxes that have less than 100 profiles for each October month are masked. The gray area represents the perennial mask and is excluded from our study. CALIPSO–GOCCP instantaneous profiles within the intermittent mask are split into over open water (footprint sea ice concentration $< 15\%$) and over sea ice (footprint sea ice concentration $> 80\%$). The white area represents the intermittent mask where the surface is mixed with open water and sea ice (footprint sea ice concentration $> 15\%$ and $< 80\%$) and is excluded from our study hereafter. The grid boxes with less than 5 years of data over a given surface type are dashed in the interannual means. Averages established over the intermittent mask, including the dashed area, are reported in parentheses. (c) Distribution of the surface LW cloud radiative effect (CRE) within the intermittent mask over open water (blue; when the footprint sea ice concentration $< 15\%$) and over sea ice (cyan; when the footprint sea ice concentration $> 80\%$). The solid line represents the surface LW Opaque CRE and the dashed line represents the surface LW Thin CRE. The CREs are normalized by the number of profiles over each surface type for each year. The color-shaded regions are the interannual variance around the interannual mean of surface LW CRE distributions over each surface type and for each cloud type. The gray-shaded vertical bar delimits low-level and high-level opaque clouds. Data are collected during October months between 2008–2020 period from LWCRE–LIDAR (Arouf, Chepfer, Vaillant de Guélis, Chiriaco, et al., 2022) on local instantaneous scale.

over open water than they do over sea ice. Specifically, large surface longwave cloud warming values (*i.e.* surface LW CRE values $> 80\,\mathrm{W\ m^{-2}}$) are much more frequent ($\sim$+50%) over open water than over sea ice and are caused by low-level opaque clouds. For thin clouds, even though they are numerous at averaged altitudes lower than 2 km, they warm less the surface with surface longwave cloud warming ranging from 0 to $40\,\mathrm{W\ m^{-2}}$.

Comparing October with November, a month with less open water in the observational record (Figure 4b-d), shows that like October, November also has more low-level

opaque clouds over open water than over sea ice within the November intermittent mask (not shown). The low-level opaque cloud cover differences over sea ice and over open water are 12% in October and 24% in November. Therefore, even though November has a lot more sea ice within the intermittent mask (59% in November Vs 31% in October), the low-level opaque cloud cover differences seen in October persist into November. Consistent with these low-level opaque cloud cover differences, there are also more very large surface longwave cloud warming (*i.e.* surface LW CRE values $> 80\,\mathrm{W\ m^{-2}}$) over open water than over sea ice. But, unlike October, the occurrence frequency difference is even larger in November. In November, large surface longwave cloud warming (*i.e.* surface LW CRE values $> 80\,\mathrm{W\ m^{-2}}$) occur $\sim$+200% more frequently over open water than over sea ice.

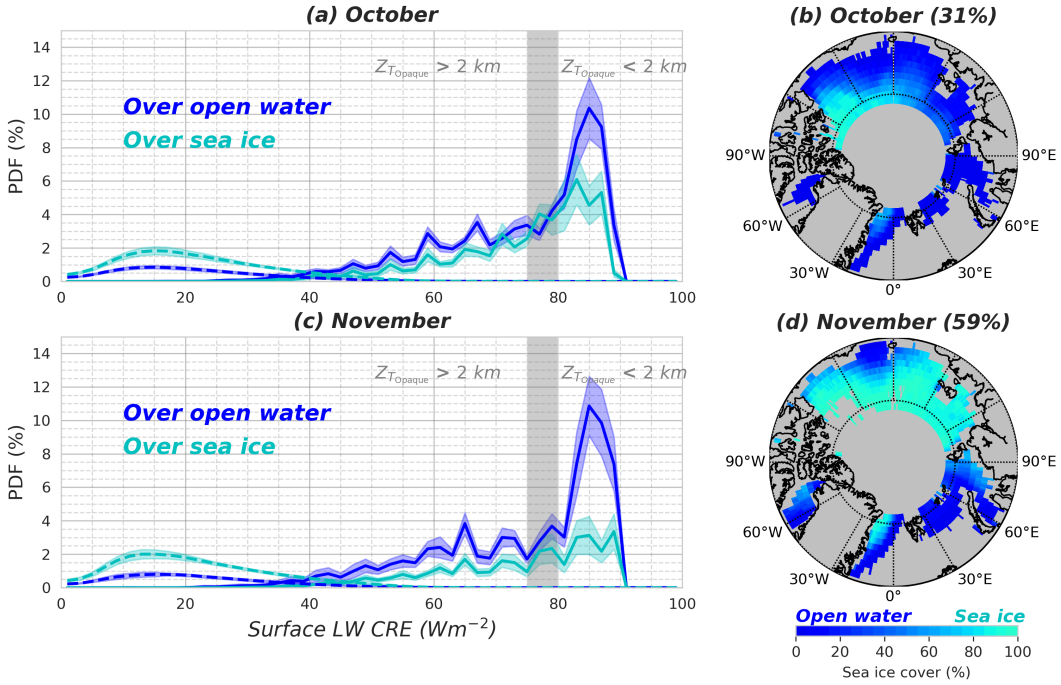

Figure 4. (a) same as Figure 3c, (b) same as Figure (a) but for November months over the November intermittent mask. (c–d) maps of the sea ice cover within the intermittent masks for October and November months respectively. The gray area represents the perennial mask and is excluded from our study. Averages established over the intermittent masks are reported in parentheses. Data are collected between 2008–2020 period for October months (1^{st} line) and November months (2^{nd} line).

5 Discussion and conclusions

Our results suggest that clouds could lengthen the melt season by delaying sea ice freeze-up. We show that low-level opaque clouds formed over newly open water warm the surface during late fall. These low-level opaque clouds are dominant in regions where sea ice varies (intermittent mask) and are more numerous over open water than over sea ice. We found that large surface longwave cloud warming occurs $\sim$+50% more often over open water than over sea ice during October months. During November compared to October, we found an even higher increase of large surface longwave cloud warming over open water than over sea ice. Thus, low-level opaque clouds warm the surface $\sim$+200% more often over open water than over sea ice during November.

Uncertainties in the surface longwave cloud warming would not change the overall results drawn in this study. Specifically, uncertainties in the surface longwave cloud warming might be induced by the space lidar not seeing the opaque cloud base. The average altitude of opaque clouds ($Z_{T_{Opaque}}$) would be lower if the cloud base is documented better. Therefore, the surface longwave cloud warming would be larger. The space lidar missing the cloud base height results in less occurrence of large surface longwave cloud warming. Said differently, large surface longwave cloud warming would occur even more frequently than +50% over open water compared to over sea ice during October months if the space lidar documents better cloud base height and would emphasize more the fact that large surface longwave cloud warming occurs more frequently over open water than over sea ice. ∼6% of CALIPSO profiles are classified as uncertain and are excluded from our study but their percentage remains small to change drastically our results. Adding to this, ∼25% of all CALIPSO profiles occur over mixed surface types during October months and are excluded from our study when we split CALIPSO's profiles into over open water and over sea ice.

Our results suggest even more large surface longwave cloud warming as the Arctic goes ice-free. Indeed, during the last two decades, sea ice has been subject to more melt and longer melt seasons with quite a lot of variability (Serreze & Meier, 2019), *i.e.* early melt season onset and a delay in the freeze-up season leaving more open water later into the fall. As the Arctic warms, the melt season is expected to lengthen further (Stroeve et al., 2014) leading to more open water in late fall. Future November may look more like actual October and future December may look like actual November with a huge increase in the occurrence of large surface longwave cloud warming over open water than over sea ice. Said in other words, more open water extent as the Arctic goes sea ice-free in the future (Pistone et al., 2019) combined with ocean-atmosphere coupling during non-summer seasons, will promote low-level cloud formation (Kay & Gettelman, 2009; Palm et al., 2010; Sato et al., 2012) leading to more large surface cloud warming.

To sum up, our study helps to improve our understanding of cloud influence on surface energy budget during late fall as Arctic sea ice retreats. It quantifies the surface longwave warming induced by low-level clouds as sea ice retreats and suggests that clouds would help to lengthen the melt season by potentially delaying sea ice freeze-up.

Acknowledgments

We are grateful to Airbus for contributing to the funding of the first author PhD grant. We thank NASA/CNES for the CALIPSO level-1 data and the Mesocentre ESPRI/IPSL for the computational resources. We recognize the support of CNES for the development of the CALIPSO–GOCCP product. Contributions of JEK and TSL were funded by NASA CloudSat/CALIPSO Science Team grant 80NSSC20K0135.

Open Research

The LWCRE–LIDAR–Ed1 is available for the 2008–2020 time period at doi.org/10.14768/70d5f4b5-e740-4d4c-b1ec-f6459f7e5563 for the monthly 2°×2° gridded dataset (Arouf, Chepfer, Vaillant de Guélis, Guzman, et al., 2022), and at doi.org/10.14768/d4de28c3-0912-4244-8c2b-6fe259eb863c for the dataset along orbit track. The 2BFLX monthly 2.5° × 2.5° dataset for the 2007−2010 time period is described at https://www.cloudsat.cira.colostate.edu/data-products/2b-flxhr-lidar and users can create a free account to order the data at this link https://www.cloudsat.cira.colostate.edu/accounts/login/?next=/order/ . The NSIDC sea ice extent dataset is available on doi.org/10.7265/N5K072F8 (Fetterer et al., 2017).

References

Agnew, T., & Howell, S. (2003). The use of operational ice charts for evaluating pas-

sive microwave ice concentration data. *Atmosphere-ocean*, *41*(4), 317–331. doi: 10.3137/ao.410405

Arouf, A., Chepfer, H., Vaillant de Guélis, T., Chiriaco, M., Shupe, M. D., Guzman, R., ... Gallagher, M. R. (2022). The surface longwave cloud radiative effect derived from space lidar observations. *Atmospheric Measurement Techniques*, *15*, 3893–3923. doi: 10.5194/amt-15-3893-2022

Arouf, A., Chepfer, H., Vaillant de Guélis, T., Guzman, R., Feofilov, A., & Raberanto, P. (2022). *Longwave cloud radiative effect derived from space lidar observations at the surface and toa – edition 1: Monthly gridded product* [dataset]. IPSL. doi: 10.14768/70d5f4b5-e740-4d4c-b1ec-f6459f7e5563

Cesana, G., Kay, J. E., Chepfer, H., English, J. M., & de Boer, G. (2012). Ubiquitous low-level liquid-containing Arctic clouds: New observations and climate model constraints from CALIPSO-GOCCP. *Geophysical Research Letters*, *39*(20). doi: 10.1029/2012GL053385

Chepfer, H., Bony, S., Winker, D., Cesana, G., Dufresne, J. L., Minnis, P., ... Zeng, S. (2010). The GCM-Oriented CALIPSO Cloud Product (CALIPSO-GOCCP). *Journal of Geophysical Research*, *115*, D00H16. doi: 10.1029/2009JD012251

Chepfer, H., Noel, V., Winker, D., & Chiriaco, M. (2014). Where and when will we observe cloud changes due to climate warming? *Geophysical Research Letters*, *41*(23), 8387–8395. doi: 10.1002/2014GL061792

Fetterer, F., Knowles, K., Meier, W. N., Savoie, M., & Windnagel., A. K. (2017). *Sea ice index, version 3.* National Snow and Ice Data Center. doi: 10.7265/N5K072F8

Guzman, R., Chepfer, H., Noel, V., Vaillant de Guélis, T., Kay, J. E., Raberanto, P., ... Winker, D. M. (2017). Direct atmosphere opacity observations from CALIPSO provide new constraints on cloud-radiation interactions. *Journal of Geophysical Research: Atmospheres*, *122*, 1066–1085. doi: 10.1002/2016JD025946

Henderson, D. S., L'Ecuyer, T., Stephens, G., Partain, P., & Sekiguchi, M. (2013). A Multisensor Perspective on the Radiative Impacts of Clouds and Aerosols. *Journal of Applied Meteorology and Climatology*, *52*, 853–871. doi: 10.1175/JAMC-D-12-025.1

Huang, Y., Dong, X., Bailey, D. A., Holland, M. M., Xi, B., DuVivier, A. K., ... Deng, Y. (2019). Thicker Clouds and Accelerated Arctic Sea Ice Decline: The Atmosphere-Sea Ice Interactions in Spring. *Geophysical Research Letters*, *46*(12), 6980–6989. doi: 10.1029/2019GL082791

Kay, J. E., & Gettelman, A. (2009). Cloud influence on and response to seasonal Arctic sea ice loss. *Journal of Geophysical Research*, *114*, D18204. doi: 10.1029/2009JD011773

Kay, J. E., & L'Ecuyer, T. (2013). Observational constraints on Arctic Ocean clouds and radiative fluxes during the early 21st century. *Journal of Geophysical Research: Atmospheres*, *118*, 7219–7236. doi: 10.1002/jgrd.50489

L'Ecuyer, T. S., Hang, Y., Matus, A. V., & Wang, Z. (2019). Reassessing the Effect of Cloud Type on Earth's Energy Balance in the Age of Active Spaceborne Observations. Part I: Top of Atmosphere and Surface. *Journal of Climate*, *32*(19), 6197–6217. doi: 10.1175/JCLI-D-18-0753.1

Manabe, S., & Stouffer, R. J. (1980). Sensitivity of a global climate model to an increase of CO2 concentration in the atmosphere. *Journal of Geophysical Research: Oceans*, *85*(C10), 5529–5554. doi: 10.1029/JC085iC10p05529

Matus, A. V., & L'Ecuyer, T. S. (2017). The role of cloud phase in Earth's radiation budget: CLOUD PHASE IN EARTH'S RADIATION BUDGET. *Journal of Geophysical Research: Atmospheres*, *122*, 2559–2578. doi: 10.1002/2016JD025951

Morrison, A. L., Kay, J. E., Chepfer, H., Guzman, R., & Yettella, V. (2018). Isolating the Liquid Cloud Response to Recent Arctic Sea Ice Variability Using

Spaceborne Lidar Observations. *Journal of Geophysical Research: Atmospheres*, *123*, 473–490. doi: 10.1002/2017JD027248

Nolin, A., Armstrong, R., & Maslanik, J. (1998). Near-real-time SSM/I-SSMIS EASE-Grid daily global ice concentration and snow extent, version 4. *NASA National Snow and Ice Data Center Distributed Active Archive Center*, *10*. doi: 10.5067/VF7QO90IHZ99

Palm, S. P., Strey, S. T., Spinhirne, J., & Markus, T. (2010). Influence of arctic sea ice extent on polar cloud fraction and vertical structure and implications for regional climate. *Journal of Geophysical Research: Atmospheres*, *115*(D21). doi: 10.1029/2010JD013900

Pistone, K., Eisenman, I., & Ramanathan, V. (2019). Radiative heating of an ice-free arctic ocean. *Geophysical Research Letters*, *46*, 7474–7480. doi: 10.1029/2019GL082914

Rantanen, M., Karpechko, A. Y., Lipponen, A., Nordling, K., Hyvärinen, O., Ruosteenoja, K., ... Laaksonen, A. (2022). The Arctic has warmed nearly four times faster than the globe since 1979. *Communications Earth & Environment*, *3*(1), 1–10. doi: 10.1038/s43247-022-00498-3

Sato, K., Inoue, J., Kodama, Y.-M., & Overland, J. E. (2012). Impact of arctic sea-ice retreat on the recent change in cloud-base height during autumn. *Geophysical Research Letters*, *39*(10). doi: 10.1029/2012GL051850

Serreze, M. C., & Barry, R. G. (2011). Processes and impacts of Arctic amplification: A research synthesis. *Global and Planetary Change*, *77*, 85–96. doi: 10.1016/j.gloplacha.2011.03.004

Serreze, M. C., & Meier, W. N. (2019). The Arctic's sea ice cover: trends, variability, predictability, and comparisons to the Antarctic. *Annals of the New York Academy of Sciences*, *1436*(1), 36–53. doi: 10.1111/nyas.13856

Shupe, M. D., & Intrieri, J. M. (2004). Cloud Radiative Forcing of the Arctic Surface: The Influence of Cloud Properties, Surface Albedo, and Solar Zenith Angle. *Journal of Climate*, *17*, 616–628. doi: 10.1175/1520-0442(2004)017⟨0616:CRFOTA⟩2.0.CO;2

Stroeve, J. C., Markus, T., Boisvert, L., Miller, J., & Barrett, A. (2014). Changes in Arctic melt season and implications for sea ice loss. *Geophysical Research Letters*, *41*, 1216–1225. doi: 10.1002/2013GL058951

Stroeve, J. C., Serreze, M. C., Holland, M. M., Kay, J. E., Malanik, J., & Barrett, A. P. (2012). The Arctic's rapidly shrinking sea ice cover: a research synthesis. *Climatic Change*, *110*, 1005–1027. doi: 10.1007/s10584-011-0101-1

Stubenrauch, C. J., Rossow, W. B., Kinne, S., Ackerman, S., Cesana, G., Chepfer, H., ... Zhao, G. (2013). Assessment of global cloud datasets from satellites: Project and database initiated by the GEWEX radiation panel. *Bulletin of the American Meteorological Society*, *94*, 1031–1049. doi: 10.1175/BAMS-D-12-00117.1

Vaillant de Guélis, T., Chepfer, H., Noel, V., Guzman, R., Dubuisson, P., Winker, D. M., & Kato, S. (2017). The link between outgoing longwave radiation and the altitude at which a spaceborne lidar beam is fully attenuated. *Atmospheric Measurement Techniques*, *10*, 4659–4685. doi: 10.5194/amt-10-4659-2017

Winker, D. M., Pelon, J., Coakley, J. A., Ackerman, S. A., Charlson, R. J., Colarco, P. R., ... Wielicki, B. A. (2010). The CALIPSO mission: A global 3d view of aerosols and clouds. *Bulletin of the American Meteorological Society*, *91*, 1211–1229. doi: 10.1175/2010BAMS3009.1

Figure 1.

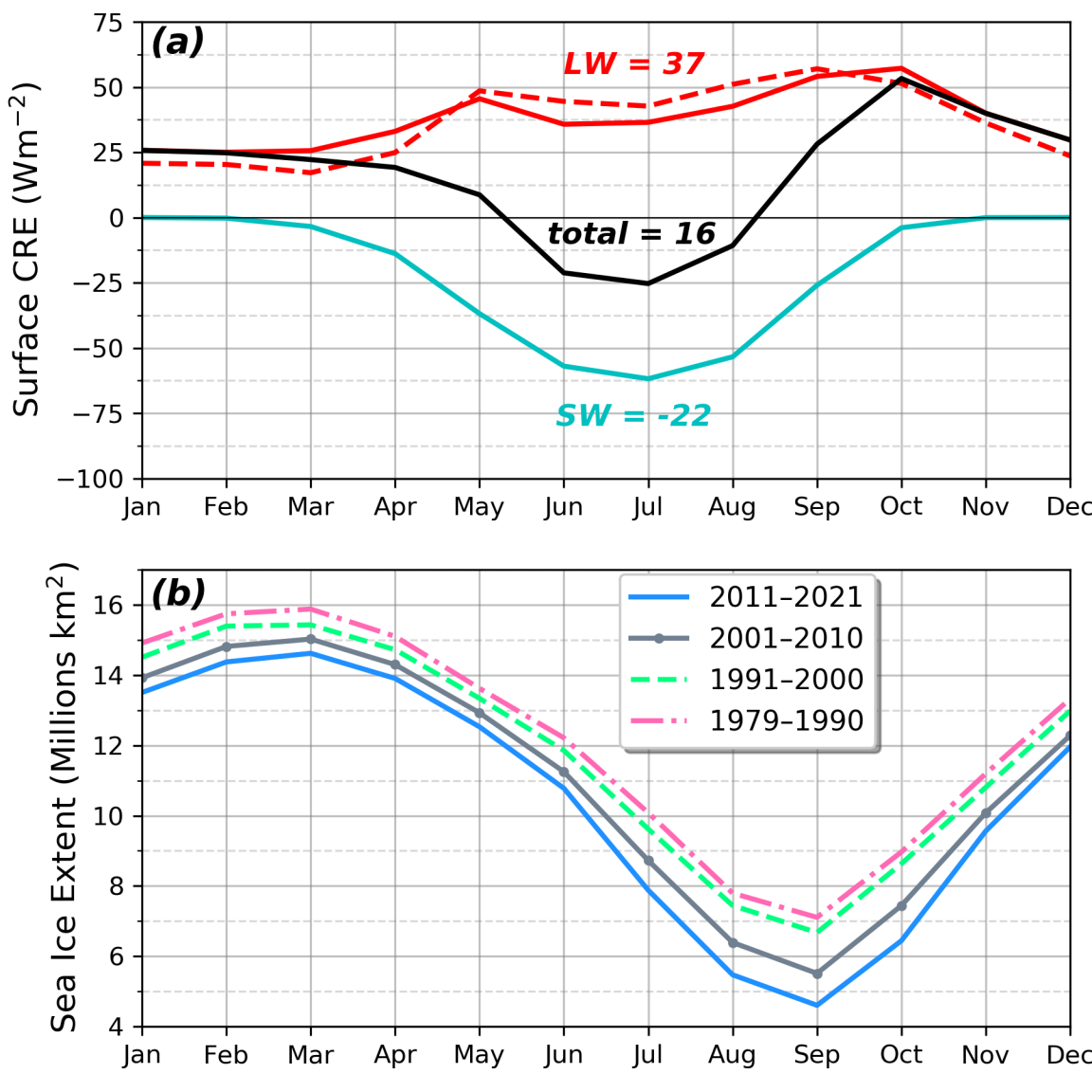
(a)
LW = 37
total = 16
SW = -22
Surface CRE (Wm^{-2})
75
50
25
0
−25
−50
−75
−100
Jan
Feb
Mar
Apr
May
Jun
Jul
Aug
Sep
Oct
Nov
Dec
(b)
2011–2021
2001–2010
1991–2000
1979–1990
Sea Ice Extent (Millions km^2)
16
14
12
10
8
6
4

Figure 2.

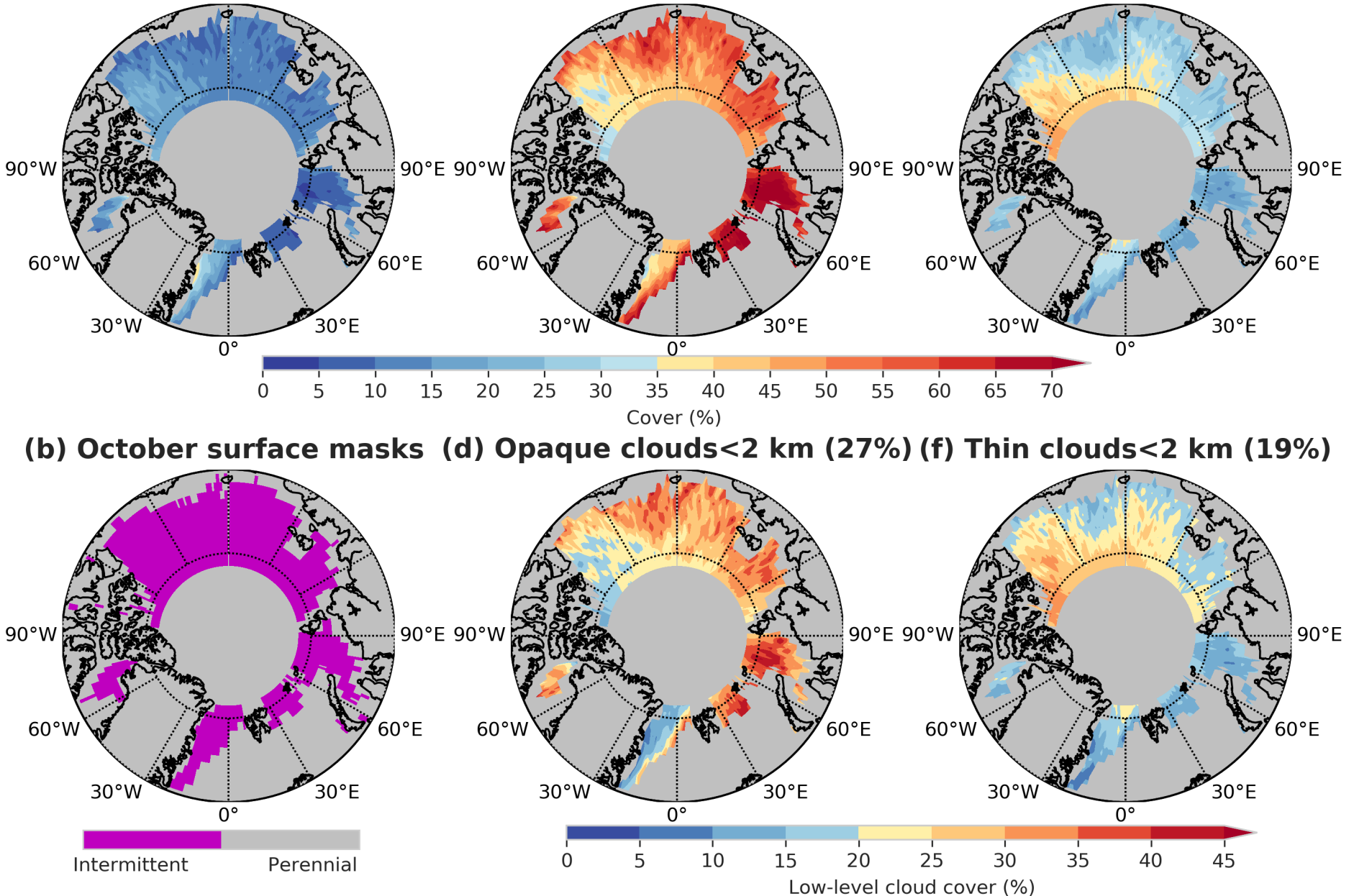
(a) Clear sky (13%)
(c) All Opaque clouds (52%)
(e) All Thin clouds (29%)
90°W
90°E
60°W
60°E
30°W
30°E
0°
0 5 10 15 20 25 30 35 40 45 50 55 60 65 70
Cover (%)
(b) October surface masks
(d) Opaque clouds<2 km (27%)
(f) Thin clouds<2 km (19%)
Intermittent
Perennial
0 5 10 15 20 25 30 35 40 45
Low-level cloud cover (%)

Figure 3.

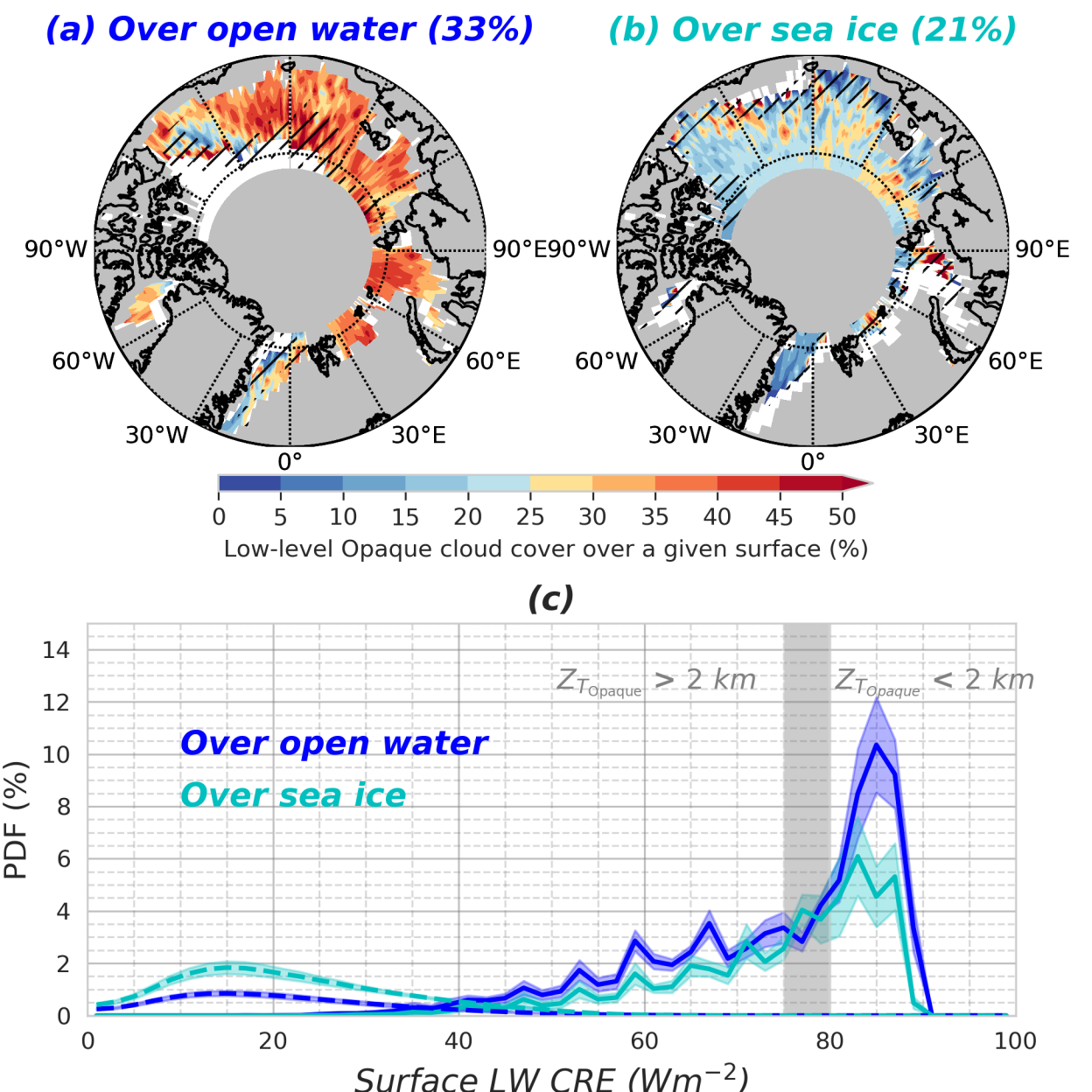
(a) Over open water (33%)
(b) Over sea ice (21%)
90°W
90°E
60°W
60°E
30°W
30°E
0°
0
5
10
15
20
25
30
35
40
45
50
Low-level Opaque cloud cover over a given surface (%)
(c)
$Z_{T_{Opaque}}$ > 2 km
$Z_{T_{Opaque}}$ < 2 km
Over open water
Over sea ice
PDF (%)
0
2
4
6
8
10
12
14
0
20
40
60
80
100
Surface LW CRE (Wm^{-2})

Figure 4.

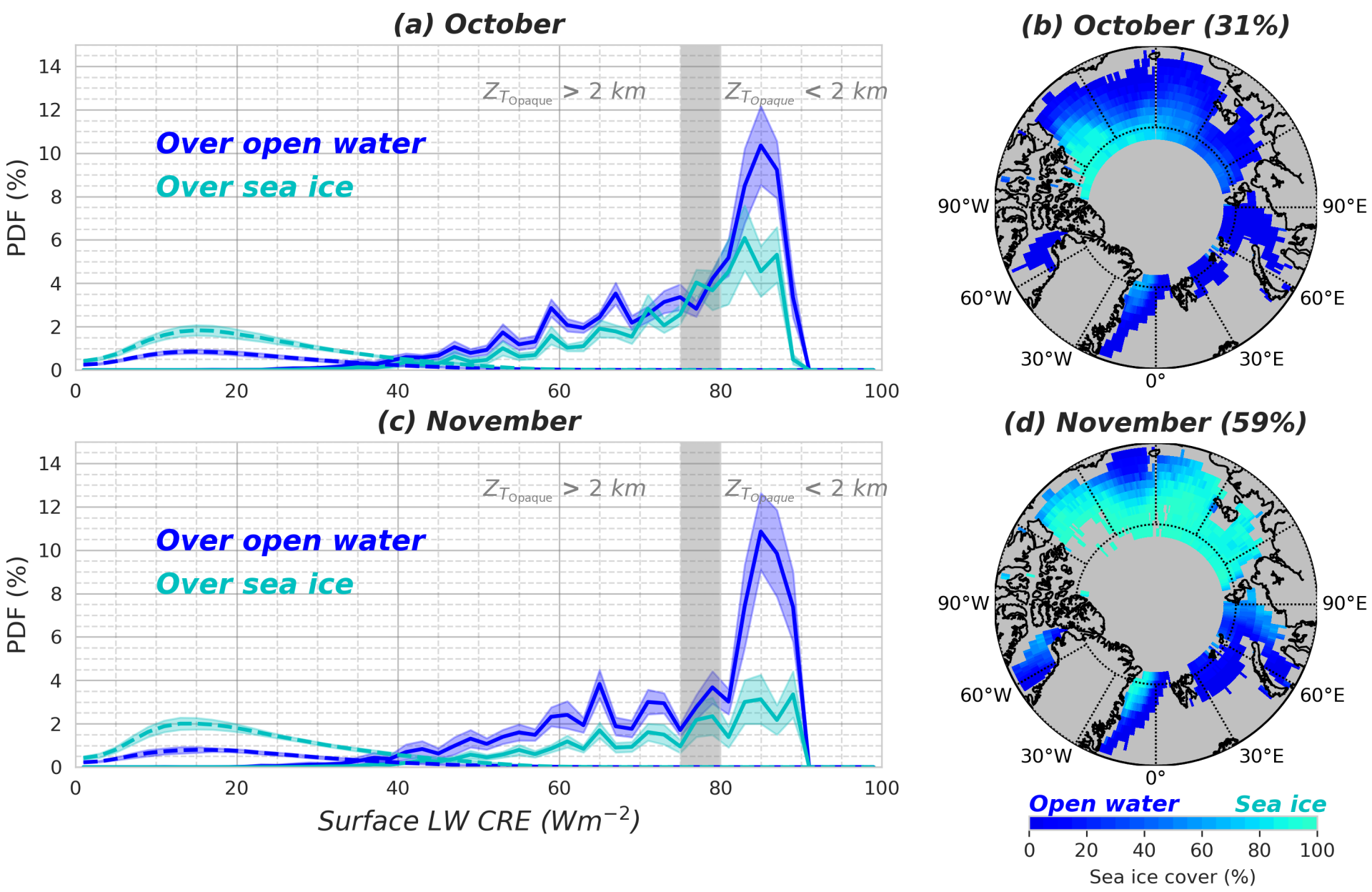
(a) October
(b) October (31%)
(c) November
(d) November (59%)
$Z_{T_{Opaque}}$ > 2 km
$Z_{T_{Opaque}}$ < 2 km
Over open water
Over sea ice
PDF (%)
Surface LW CRE (Wm^{-2})
90°W
90°E
60°W
60°E
30°W
30°E
0°
Open water
Sea ice
Sea ice cover (%)